Outdoor MIMO Wireless Channels: Models and Performance Prediction

David Gesbert, *Member, IEEE*, Helmut Bölcskei, *Member, IEEE*, Dhananjay A. Gore, and Arogyaswami J. Paulraj, *Fellow, IEEE*

***Abstract*—We present a new model for multiple-input–multiple-output (MIMO) outdoor wireless fading channels and their capacity performance. The proposed model is more general and realistic than the usual independent and identically distributed (i.i.d.) model, and allows us to investigate the behavior of channel capacity as a function of the scattering radii at transmitter and receiver, distance between the transmit and receive arrays, and antenna beamwidths and spacing. We show how MIMO capacity is governed by spatial fading correlation and the condition number of the channel matrix through specific sets of propagation parameters. The proposed model explains the existence of "pinhole" channels which exhibit low spatial fading correlation at both ends of the link but still have poor rank properties, and hence, low ergodic capacity. In fact, the model suggests the existence of a more general family of channels spanning continuously from full rank i.i.d. to low-rank pinhole cases. We suggest guidelines for predicting high rank (and hence, high ergodic capacity) in MIMO channels, and show that even at long ranges, high channel rank can easily be sustained under mild scattering conditions. Finally, we validate our results by simulations using ray tracing techniques. Connections with basic antenna theory are made.**

***Index Terms*—Antenna arrays, channel capacity, channel modeling, diversity, multiple-input–multiple-output channels, smart antennas, space–time coding, spatial multiplexing.**

I. Introduction

THE PROSPECT of extraordinary improvements in the capacity of wireless networks has drawn considerable attention to multiple-input–multiple-output (MIMO) communication techniques. MIMO methods make use of multi-element antenna arrays at both the transmit and the receive side of a radio link to drastically improve the capacity over more traditional single-input–multiple-output (SIMO) systems (with multiple antennas typically being used at the base station only) [1], [5], [8], [27]. SIMO channels can provide *diversity gain*, *array gain*, and *interference canceling gain*. In addition to these advantages, MIMO links can offer a so-called *multiplexing gain* by opening parallel spatial data pipes or channels within the same frequency band at no additional power expenditure. In the presence of rich multipath leading to antenna decorrelation and full channel rank, MIMO links offer capacity gains that are proportional to the minimum of the number of transmit and receive antennas [10]. These gains can be achieved using spatial multiplexing algorithms (a.k.a. "BLAST") [1], [2], [8], [9], [26], [27]. In the presence of channel rank loss one resorts to more robust lower rate transmission techniques based on space–time codes [16], [17], [28].

1) Previous Work and Open Problems: Although a profound understanding of MIMO channels is crucial in selecting proper signaling strategies in MIMO wireless networks, the literature on realistic MIMO channel models remains scarce. Measurements of outdoor MIMO channels have been reported in [18]–[21] without always providing insights into the relation between the channel structure, the corresponding capacity, and the propagation environment. For the line-of-sight (LOS) case, specific arrangements of antenna arrays at the transmitter and the receiver maximizing the orthogonality between antenna signatures (and hence, the capacity) have been reported in [15]. A detailed treatment of array gain and capacity of MIMO channels for the case where both the transmitter and the receiver know the channel can be found in [7]. In the fading case, previous studies have mostly been confined to independent and identically distributed (i.i.d.) Gaussian channels, an idealistic assumption where the entries of the channel matrix are modeled as independent complex Gaussian random variables (see, e.g., [10]). The influence of spatial fading correlation at either the transmit or the receive side of a wireless MIMO radio link has been addressed in [22], [23], and [27]. While the models used in [22] and [27], for example, are simple and allow us to gain insight into the impact of propagation conditions on MIMO capacity, they assume that only spatial fading correlation is responsible for the rank structure of the MIMO channel. In practice, however, the realization of high MIMO capacity in actual radio channels is sensitive not only to the fading correlation, but also to the structure of scattering in the propagation environment. In the existing literature, high-rank behavior has only loosely been linked to the existence of a dense scattering environment. Aforementioned results of measurements in urban settings tend to corroborate this behavior. However, several key questions regarding outdoor MIMO channels remain open.

- What is the capacity of a typical outdoor MIMO channel?
- What are the key propagation parameters governing the capacity behavior?

Paper approved by M. Z. Win, the Editor for Equalization and Diversity of the IEEE Communications Society. Manuscript received August 30, 2000; revised March 27, 2002. The work of H. Bölcskei was supported in part by the Austrian National Science Foundation (FWF) under Grant J1868-TEC. This paper was presented in part at IEEE Globecom 2000, San Francisco, CA, November 2000, and at the Asilomar Conference on Signals, Systems, and Computers, Pacific Grove, CA, October 2000.

D. Gesbert is with the Department of Informatics, University of Oslo, 0316 Oslo, Norway (e-mail: gesbert@ifi.uio.no).

H. Bölcskei is with the Communication Technology Laboratory, Swiss Federal Institute of Technology (ETH) Zurich, CH-8092 Zürich, Switzerland (e-mail: boelcskei@nari.ee.ethz.ch).

D. A. Gore and A. J. Paulraj are with the Information Systems Laboratory, Department of Electrical Engineering, Stanford University, Stanford, CA 94305-9510 USA (e-mail: dagore@stanford.edu; apaulraj@stanford.edu).

Digital Object Identifier 10.1109/TCOMM.2002.806555

- Under what conditions do we get a high-rank MIMO channel (and hence, high capacity)?
- What is a simple analytical model describing the capacity behavior of outdoor MIMO wireless channels accurately?

2) Summary of Contributions and Relation to Previous Work: In this paper, we address the above-mentioned questions, and more generally, problems related to the prediction of the capacity of outdoor MIMO channels. We start with theoretical model concepts and illustrate their capacity behavior. We then suggest a simple classification of MIMO channels and devise a MIMO channel model which is general enough to encompass many cases of practical relevance. The channel model used in [22] and [27] does not encompass important propagation scenarios such as the uncorrelated low-rank and correlated low-rank channel models presented in Section II. Another difference in the present channel model is that correlation is allowed at both the transmitter and the receiver. Finally, a fundamental difference between the new model and previous models proposed in the literature is that the impact of spatial fading correlation and channel rank are decoupled, although not fully independent. This allows us, for example, to describe MIMO channels with uncorrelated spatial fading at the transmitter and the receiver, but reduced channel rank (and hence, small ergodic capacity). Such channels will be referred to as "pinhole" channels, and have independently been shown to arise in specific roof-top diffraction scenarios [6], [24]. We demonstrate that the pinhole channel is, in fact, a special member of a much broader class of MIMO channels.

3) Organization of the Paper: In Section II, we provide a brief review of the capacity formula for MIMO channels, followed by a new classification of MIMO fading channels. Section III is devoted to the case of deterministic MIMO channels in a green field (i.e., nonscattering) environment and presents a simple condition guaranteeing high rank (and hence, high capacity). Connections with well-known single antenna theory results are made. In Section IV, we turn to scattering situations and introduce a stochastic channel model describing the capacity behavior as a function of the wavelength, the scattering radii at the transmitter and the receiver, the distance between transmit and receive arrays, antenna beamwidths, and antenna spacing. The impact of each of these parameters on capacity is interpreted and studied. Our model suggests that full MIMO capacity gain can be achieved for very realistic values of scattering radii, antenna spacing, and range. Moreover, we show that in general, antenna spacing has only a limited impact on capacity. We use the new model to predict high- and low-rank behavior of MIMO channels with potentially uncorrelated antenna fading at the transmit and receive sides. We find that channels such as the pinhole channel occur at large distances between transmitter and receiver and will rarely be observed in practice (except for the peculiar situation described in [6] and [24]). Interestingly, in the 1×1 case (i.e., one transmit and one receive antenna), the pinhole channel can be defined and yields capacities worse than the traditional Rayleigh fading channel. In Section V, our results are validated by comparing the capacity obtained from the new stochastic channel model with a ray tracing-based channel simulation where each scatterer and path is simulated. We find a good match between the two models over a wide range of situations. Finally, we conclude in Section VI.

II. Capacity of MIMO Channels and Model Classification

In this section, we briefly review the capacity formula for MIMO channels, and we present a novel classification of MIMO channels. Throughout the paper, we restrict our discussion to the frequency-flat fading case, and we assume that the transmitter has no channel knowledge, whereas the receiver has perfect channel knowledge.

A. Capacity of MIMO Channels

In what follows, we assume N transmit and M receive antennas. The instantaneous capacity (in b/s/Hz) of a stochastic MIMO channel under an average transmit power constraint is given by[1] [1], [5]

$$C = \log_2 \left[\det \left(\mathbf{I}_M + \frac{\rho}{N} \mathbf{H}\, \mathbf{H}^* \right) \right] \tag{1}$$

where $\mathbf{H}$ is the $M \times N$ channel matrix, $\mathbf{I}_M$ denotes the identity matrix of size M, and ρ is the average signal-to-noise ratio (SNR) at each receiver antenna. The elements of $\mathbf{H}$ are circularly symmetric complex Gaussian[2] with zero mean and unit variance, i.e., $[\mathbf{H}]_{m,\,n} \sim \mathcal{CN}(0,\,1)$ for $m = 1,\,2,\,\ldots,\,M$, $n = 1,\,2,\,\ldots,\,N$. Note that since $\mathbf{H}$ is random, C will be random as well. Assuming a piece-wise constant fading model (block-fading model) and coding over many independent fading intervals,[3] $C_s = \mathcal{E}_H\{C\}$ will be the Shannon (in this case, ergodic) capacity of the random MIMO channel [5]. In practice, the cumulative distribution function (cdf) of C is often used to characterize the outage properties of the MIMO channel [4].

B. Model Classification

We shall next introduce a new classification of MIMO fading channels. Although these models are theoretical in nature, this paper demonstrates them to be special cases in a broad and continuous family of MIMO channels with practical relevance.

- Uncorrelated high-rank (UHR, a.k.a., i.i.d.) model: The elements of $\mathbf{H}$ are i.i.d. $\mathcal{CN}(0,\,1)$.
- Uncorrelated low-rank (ULR) (or "pinhole") model: $\mathbf{H} = \mathbf{g}_{rx}\,\mathbf{g}_{tx}^*$, where $\mathbf{g}_{rx}$ and $\mathbf{g}_{tx}$ are independent receive and transmit fading vectors, respectively, with $\mathbf{g}_{rx} \sim \mathcal{CN}(\mathbf{0},\,\mathbf{I}_M)$ and $\mathbf{g}_{tx} \sim \mathcal{CN}(\mathbf{0},\,\mathbf{I}_N)$. In this model, every realization of $\mathbf{H}$ has rank 1, and therefore, although spatial diversity is present, ergodic capacity must be expected to be less than in the UHR model since there is no multiplexing gain. Intuitively, in this case, the diversity order is equal to $\min(M,\,N)$.
- Correlated low-rank (CLR) model: $\mathbf{H} = g_{rx} g_{tx}^* \mathbf{u}_{rx} \mathbf{u}_{tx}^*$ where $g_{rx} \sim \mathcal{CN}(0,\,1)$ and $g_{tx} \sim \mathcal{CN}(0,\,1)$ are independent scalar variables, and $\mathbf{u}_{rx}$ and $\mathbf{u}_{tx}$ are fixed deterministic vectors of size $M\times1$ and $N\times1$, respectively, and with unit modulus entries. This model yields no diversity or multiplexing gain whatsoever, just receive array gain.

[1]The superscript $*$ stands for Hermitian transpose.

[2]A circularly symmetric complex Gaussian random variable is a random variable $z = (x + jy) \sim \mathcal{CN}(0,\,\sigma^2)$, where x and y are i.i.d. $\mathcal{N}(0,\,\sigma^2/2)$.

[3]$\mathcal{E}_H$ stands for the expectation with respect to the random channel.

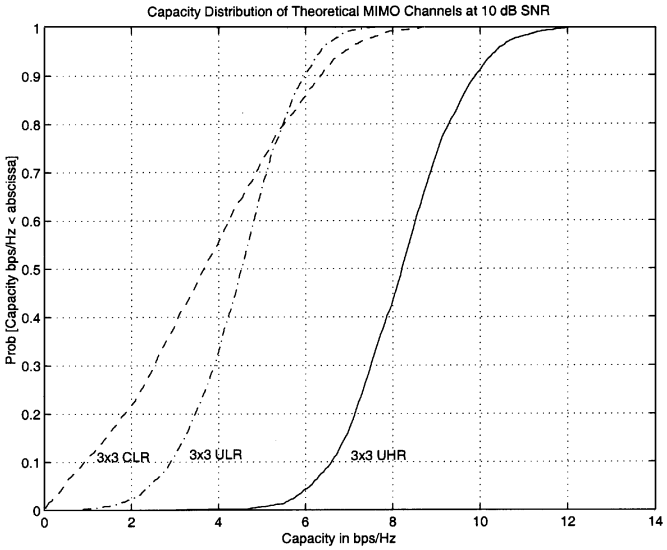

Fig. 1. ULR model shows the impact of rank loss on capacity. CLR channel loses both multiplexing and diversity gains.

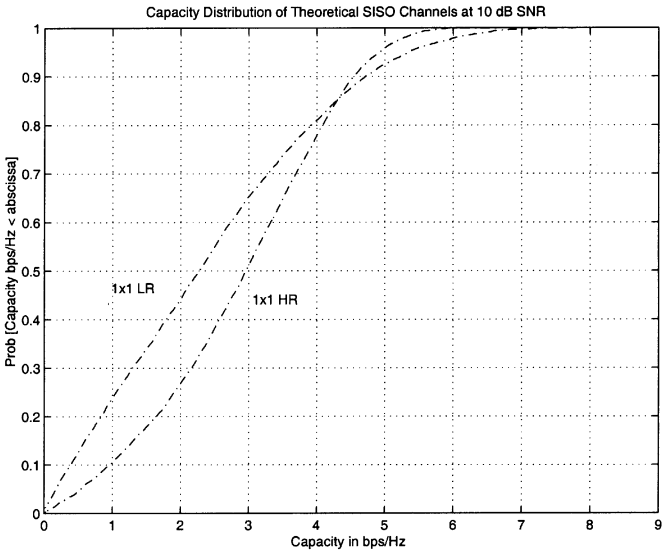

Fig. 2. Capacity curves for the 1×1 HR (Rayleigh) and 1×1 LR (double Rayleigh) channels. The double Rayleigh channel has worsened fading statistics.

We also define the following single-antenna models to which we extend the "low rank" (LR) and "high rank" (HR) concepts:

- 1×1 HR, defined by the UHR model with $M = N = 1$, also known as Rayleigh fading channel.
- 1×1 LR, defined by the ULR or CLR model with $M = N = 1$ (double Rayleigh channel).

Note that the low-rank models (ULR, CLR, 1×1 LR) above do not use the traditional normal distribution for the entries of $\mathbf{H}$, but instead the product of two Gaussian variables. This type of distribution will be shown later to occur in important practical situations.

The above models exhibit very different capacity behavior. The cdf of the corresponding capacities is depicted in Figs. 1 and 2 for $\rho = 10$ dB. Fig. 1 clearly shows the impact of rank loss on capacity. The loss in the 3×3 ULR case is due to the fact that there is only one spatial data pipe. However, in this case, much of the *diversity gain* is preserved because the antennas still fade in an uncorrelated fashion. Antenna correlation causes additional loss in capacity, which can be seen from the cdf of the 3×3 CLR channel in Fig. 1. From Fig. 2, we can conclude that the 1×1 LR model (double Rayleigh) yields less capacity than the 1×1 HR model (Rayleigh) for a wide range of outage rates. This is due to the intuitive fact that a double Rayleigh channel will fade twice as often as a standard Rayleigh channel.

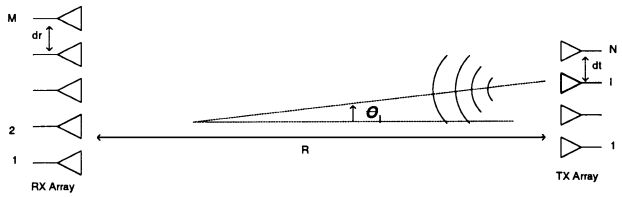

Fig. 3. N-input M-output MIMO green field model.

III. Green Field MIMO Channels

In this section, we derive conditions guaranteeing an HR MIMO channel in a green field (or LOS) environment. Concentrating on the ideal nonscattering nonfading case (i.e., deterministic channels), we suggest that rank properties are governed by simple geometrical propagation parameters. The results below are applicable in flat/rural wireless deployments. We shall see later in the paper that our findings suggest guidelines for the fading case as well.

Considering the N transmitter, M receiver setup described in Fig. 3, we assume bore-sight propagation from the transmit array to the receive array. In addition, we assume the signal radiated by the lth transmit antenna to impinge as a plane wave on the receive array at an angle of θ_l. This assumption is justified when the antenna aperture is much smaller than the range R. Finally, using the same assumption, the effect of path loss can be ignored. Denoting the signature vector induced by the lth transmit antenna as $\mathbf{h}_l = [1 e^{-2\pi j \sin(\theta_l) d_r/\lambda} \cdots e^{-2\pi j(M-1)\sin(\theta_l) d_r/\lambda}]^T$, where λ is the wavelength, and d_t and d_r are the transmit and receive antenna spacing, respectively, we have $\mathbf{H} = [\mathbf{h}_1 \mathbf{h}_2 \cdots \mathbf{h}_N]$. The common phase shift due to the distance R between transmitter and receiver has no impact on capacity and is, therefore, ignored. Clearly, when the θ_l ($l = 1, 2, \ldots, N$) (all other parameters being fixed) approach zero we find that $\mathbf{H}$ approaches the all-ones matrix, and therefore, has rank 1. In practice, this happens for large range R. As the range decreases, linear independence between the signatures starts to build up. We choose to use the full orthogonality between the signatures of adjacent pairs of transmit antennas as a criterion for the receiver to be able to separate the transmit signatures well, implying high capacity. This condition reads

$$\langle \mathbf{h}_l, \mathbf{h}_{l+1} \rangle = \sum_{m=0}^{M-1} e^{2\pi j[\sin(\theta_{l+1}) - \sin(\theta_l)] m(d_r/\lambda)} = 0. \quad (2)$$

For practical values of R, d_t, and d_r, orthogonality will occur for small θ_l. We can, therefore, set $\sin\theta_l \approx (l-1)d_t/R (l = 1, 2, \ldots, N)$. Consequently, condition (3) can be rewritten as

$$\sum_{m=0}^{M-1} e^{2\pi j m(d_t d_r/\lambda R)} = 0 \quad (3)$$

which implies

$$\frac{d_t d_r}{R} \geq \frac{\lambda}{M}. \tag{4}$$

Note that this is not sufficient to achieve exact orthogonality, although for a large number of receive antennas it will *tend* to be sufficient. In practice, for larger values of antenna spacing [larger than that imposed by (4)], the transmit antennas can fall into the grating lobes of the receive array, in which case, orthogonality is not realized. Interestingly, (4) can be rewritten into

$$\frac{\lambda}{M d_r} \leq \frac{d_t}{R} \tag{5}$$

which can be reinterpreted in terms of basic antenna theory as follows [25]. The angular resolution of the receive array (inversely proportional to the aperture in wavelengths) should be less than the angular separation between two neighboring transmitters. Of course, a similar condition in terms of transmit resolution can be obtained by enforcing orthogonality between the *rows* of $\mathbf{H}$.

In a pure LOS situation, orthogonality can only be achieved for very small values of range R. For example, at a frequency of 2 GHz with $M = 3$, a maximum of $R = 20$ m is acceptable for 1 m antenna spacing. Note that the orthogonality condition (4) depends on the number of receive antennas M only. This is so, since we are seeking separability of only the two closest transmit antennas. Clearly, linear independence of adjacent transmit antenna signatures is a necessary (but not sufficient) condition for the global channel matrix $\mathbf{H}$ to have full rank. We show later in the paper how the guideline (4) extends nicely to scattering scenarios.

IV. Distributed Scattering MIMO Model

We now turn to the case of non-line-of-sight (NLOS) channels, where fading is induced by the presence of scatterers. The purposes of this section are the following:

- to develop a stochastic MIMO channel model that captures separately the *diversity* and *rank* properties as suggested by Figs. 1 and 2;
- to suggest how the guideline offered by (4) for LOS channels can be extended to fading channels upon appropriate redefinition of d_t and d_r.

In the following, for the sake of simplicity, we consider the effect of near-field scatterers only, i.e., scatterers which are either in the vicinity (typically a few tens to hundreds of meters away) of the transmitter or the receiver. We ignore remote scatterers, assuming that the path loss will tend to limit their contribution to the overall channel. In addition, because local scatterers introduce multipath length differences which are small compared to the transmit–receive range, we assume that the quasi-common path attenuation can be factored out of the channel and focus on microscopic (Rayleigh) fading only. We also limit this particular study to a frequency-flat fading channel. The benefit of multipath delay spread in terms of increasing the rank richness of the channel was demonstrated in [3] and [27].

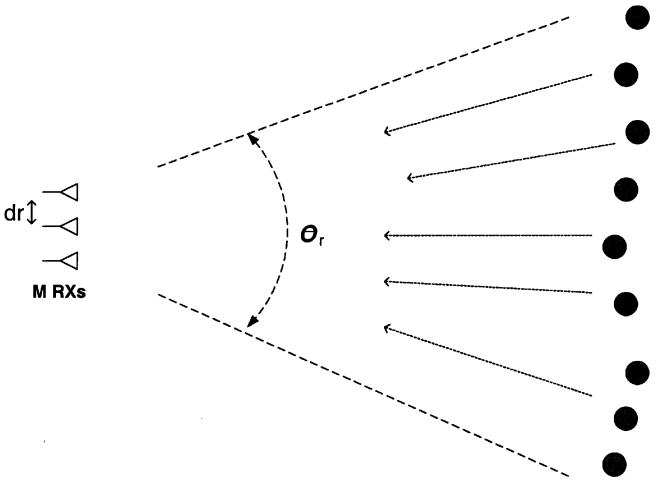

Fig. 4. Propagation scenario for SIMO fading correlation. Each scatterer transmits a plane-wave signal to a linear array.

A. SIMO Fading Correlation Model

We consider a linear receive array of M omnidirectional antennas with spacing d_r. A number of distributed scatterers in front of the array act as ideal reflectors (i.e., perfect omnidirectional scatterers) of a signal which eventually impinges on the receive array. The plane-wave directions of arrival (DOAs) of these signals span an angular spread of θ_r radians (see Fig. 4). Several distributions can be considered for the DOAs, including uniform, Gaussian, Laplacian, etc. [12]–[14]. The addition of different plane-waves causes space-selective fading at the receive antennas. It is well known that the resulting fading correlation is governed by the angle spread, the antenna spacing, and the wavelength. The receive array response vector $\mathbf{h}$ can consequently be modeled as

$$\mathbf{h} \sim \mathcal{CN}(\mathbf{0}, \mathbf{R}_{\theta_r, d_r}) \text{ or equivalently } \mathbf{h} = \mathbf{R}_{\theta_r, d_r}^{1/2}\mathbf{g} \quad \text{with} \quad \mathbf{g} \sim \mathcal{CN}(\mathbf{0}, \mathbf{I}_M) \tag{6}$$

where $\mathbf{R}_{\theta_r, d_r}$ is the $M \times M$ receive correlation matrix. Different assumptions on the statistics of the DOAs will yield different expressions for $\mathbf{R}_{\theta_r, d_r}$ [12]–[14]. For uniformly distributed DOAs, we find [12], [14]

$$[\mathbf{R}_{\theta_r, d_r}]_{m,k} = \frac{1}{S} \sum_{i=-((S-1)/2)}^{((S-1)/2)} e^{-2\pi j(k-m)d_r \cos((\pi/2)+\theta_{r,i})} \tag{7}$$

where S (odd) is the number of scatterers with corresponding DOAs $\theta_{r,i}$. For "large" values of angle spread θ_r and/or antenna spacing d_r, $\mathbf{R}_{\theta_r, d_r}$ will converge to the identity matrix, which gives uncorrelated fading. For "small" values of θ_r, d_r, the correlation matrix becomes rank deficient (eventually rank one), causing (fully) correlated fading. For the sake of simplicity, we furthermore assume the mean DOA to be orthogonal to the array (bore sight). Some comments on this model are now in order.

- **Impact of Directional Antennas:** If directional antennas are used instead of omnidirectional antennas, the effective angle spread perceived by the array can be obtained by intersecting the scattering angle spread with the main lobes of the antennas. In what follows, the directionality of

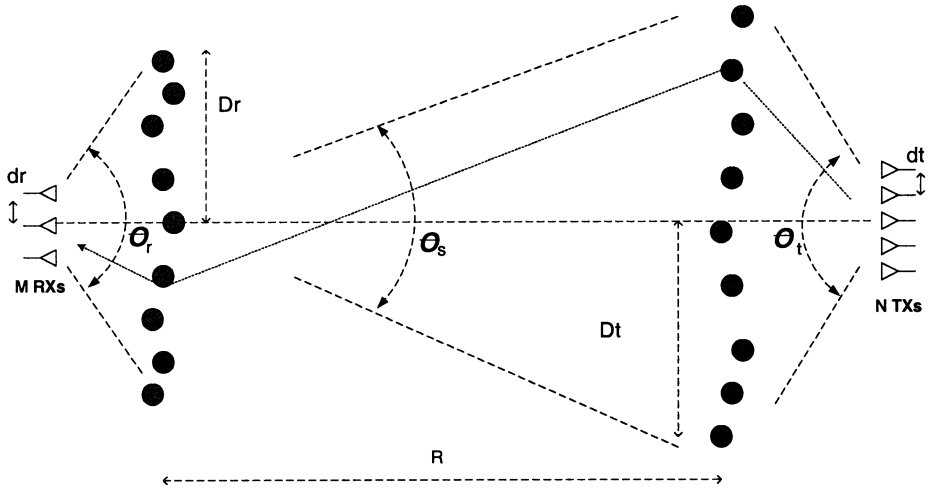

Fig. 5. Propagation scenario for fading MIMO channel. We assume plane-wave propagation. Scatterers are ideal reflectors.

antennas is accounted for by selecting the effective angle spread properly.

- **Spatial Fading Correlation at the Transmitter:** The model provided in (6) can readily be applied to an array of transmit antennas with corresponding antenna spacing and signal departure angle spread.

B. MIMO Correlated Fading Model

We now turn to the NLOS MIMO case by considering the propagation scenario depicted in Fig. 5. The propagation path between the two arrays is obstructed on both sides of the link by a set of significant near-field scatterers (such as buildings and large objects) referred to as transmit or receive scatterers. Scatterers are modeled as omnidirectional ideal reflectors. The extent of the scatterers from the horizontal axis is denoted as D_t and D_r, respectively. When omnidirectional antennas are used, D_t and D_r correspond to the transmit and receive *scattering radius*, respectively. On the receive side, the signal reflected by the scatterers onto the antennas impinge on the array with an angular spread denoted by θ_r, where θ_r is a function of the distance between the array and the scatterers. Similarly, on the transmit side we define an angular spread θ_t. In general, using directional antennas instead of omnidirectional antennas will tend to decrease the effective values of D_t and D_r and hence, the angular spreads. The scatterers are assumed to be located sufficiently far from the antennas for the plane-wave assumption to hold. We furthermore assume that $D_t \ll R$ and $D_r \ll R$ (local scattering condition).

1) Signal at the Receive Scatterers: We assume S scatterers on both sides, where S is an arbitrary, large enough number for random fading to occur (typically $S > 10$ is sufficient). The exact locations of the scatterers are irrelevant here. Every transmit scatterer captures the radio signal and reradiates it in the form of a plane wave toward the receive scatterers, which are viewed as an array of S virtual antennas with average spacing $2D_r/S$, and as such, experience an angle spread defined by $\tan(\theta_S/2) = D_t/R$. We denote the vector signal originating from the nth transmit antenna and captured by the S receive scatterers as $\mathbf{y}_n = [y_{1,n}\ y_{2,n}\ \ldots y_{S,n}]^T$. Approximating the receive scatterers as a uniform array of sensors and using the correlation model of (6), we find

$$\begin{aligned}&\mathbf{y}_n \sim \mathcal{CN}(\mathbf{0},\, \mathbf{R}_{\theta_S,\,2D_r/S}) \text{ or equivalently}\\ &\mathbf{y}_n = \mathbf{R}^{1/2}_{\theta_S,\,2D_r/S}\mathbf{g}_n \quad \text{with}\\ &\mathbf{g}_n \sim \mathcal{CN}(\mathbf{0},\, \mathbf{I}_S).\end{aligned} \tag{8}$$

For uncorrelated transmit antennas, the $S \times N$ matrix describing the propagation between the N transmit antennas and the S receive scatterers simply writes

$$\mathbf{Y} = [\mathbf{y}_1\ \mathbf{y}_2\ \cdots\ \mathbf{y}_N] = \mathbf{R}^{1/2}_{\theta_S,\,2D_r/S}\mathbf{G}_t \tag{9}$$

where $\mathbf{G}_t = [\mathbf{g}_1\ \mathbf{g}_2\ \cdots\ \mathbf{g}_N]$ is an $S \times N$ i.i.d. Rayleigh fading matrix. However, there is generally correlation between the transmit antennas because of finite angle spread and insufficient antenna spacing. Therefore, a more appropriate model becomes

$$\mathbf{Y} = \mathbf{R}^{1/2}_{\theta_S,\,2D_r/S}\ \mathbf{G}_t\ \mathbf{R}^{1/2}_{\theta_t,\,d_t} \tag{10}$$

where $\mathbf{R}^{1/2}_{\theta_t,\,d_t}$ is the $N \times N$ matrix controlling the transmit antenna correlation as suggested in the transmit form of (6).

2) MIMO Model: Like the transmit scatterers, the receiver scatterers are assumed to ideally reradiate the captured energy. As shown in Fig. 5, a set of plane waves, with total angle spread θ_r, impinge on the receive array. Denoting the distance between the sth scatterer and the mth receive antenna as $d_{s,\,m}$, the vector of received signals from the nth transmit antenna can be written as

$$\mathbf{z}_n = \underbrace{\begin{bmatrix} e^{-2\pi j d_{1,\,1}/\lambda} & \cdots & e^{-2\pi j d_{S,\,1}/\lambda} \\ \vdots & & \vdots \\ e^{-2\pi j d_{1,\,M}/\lambda} & \cdots & e^{-2\pi j d_{S,\,M}/\lambda} \end{bmatrix}}_{\mathbf{\Phi}} \mathbf{y}_n. \tag{11}$$

Collecting all receive and transmit antennas according to $\mathbf{Z} = [\mathbf{z}_1\ \mathbf{z}_2\ \cdots\ \mathbf{z}_N]$, we obtain the following MIMO channel model:

$$\mathbf{Z} = \mathbf{\Phi}\mathbf{Y}. \tag{12}$$

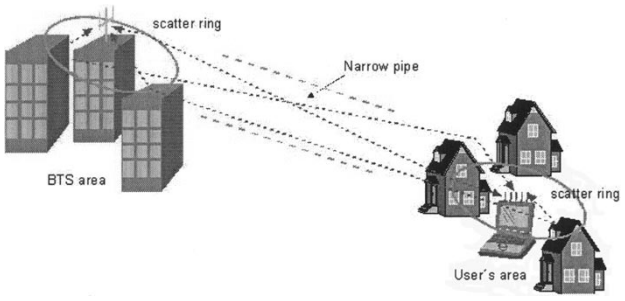

Fig. 6. Example of pinhole realization. Reflections around the base transmitter stations and subscribers cause locally uncorrelated fading. However, because the scatter rings are too small compared to the separation between the two rings, the channel rank is low.

The problem with the expression in (12) is the explicit use of deterministic phase shifts in the matrix $\mathbf{\Phi}$ which makes the model inconvenient. The simple equivalence result below allows us to get rid of this inconvenience and obtain a fully stochastic, hence simpler, MIMO channel model.

Lemma: For $S \to \infty$, $\mathbf{Z} = \mathbf{\Phi Y}$ has the same pdf as $\mathbf{R}_{\theta_r, d_r}^{1/2} \mathbf{G}_r \mathbf{Y}$, where $\mathbf{G}_r$ is an i.i.d. Rayleigh fading matrix of size $M \times S$.

Proof: See the Appendix. □

After proper power normalization[4] and replacing $\mathbf{Y}$ by (10), we obtain the following simple MIMO transfer function:

$$\mathbf{H} = \frac{1}{\sqrt{S}} \mathbf{Z} = \frac{1}{\sqrt{S}} \mathbf{R}_{\theta_r, d_r}^{1/2} \mathbf{G}_r \mathbf{R}_{\theta_S, 2D_r/S}^{1/2} \mathbf{G}_t \mathbf{R}_{\theta_t, d_t}^{1/2}. \quad (13)$$

C. Interpretation and the Pinhole Channel

The model suggested in (13) lends itself to several interesting interpretations, explaining the effect of propagation parameters on the capacity behavior of MIMO channels.

- Our model is symmetric in structure, which was to be expected from the scenario considered.
- The spatial fading correlation between the transmit antennas, and therefore, the transmit diversity gain, is governed by the deterministic matrix $\mathbf{R}_{\theta_t, d_t}^{1/2}$ and hence, implicitly by the local transmit angle spread, the transmit antenna beamwidth and spacing. On the receive side, the fading correlation is similarly controlled by the receive angle spread, antenna beamwidth, and antenna spacing through $\mathbf{R}_{\theta_r, d_r}^{1/2}$.
- Assume that fading is uncorrelated at both sides of the link (i.e., $\mathbf{R}_{\theta_t, d_t} = \mathbf{I}_N$ and $\mathbf{R}_{\theta_r, d_r} = \mathbf{I}_M$). Equation (13) shows that it is nevertheless well possible to have a rank-deficient MIMO channel with reduced capacity. Such a channel is dubbed a pinhole channel because scattering (fading) energy travels through a very thin air pipe, preventing channel rank from building up. In practice, this occurs when the rank of $\mathbf{R}_{\theta_S, 2D_r/S}^{1/2}$ drops caused by, e.g., large transmit–receive range R, or small D_t, or D_r, or both. An example of a quasi-pinhole channel is illustrated in Fig. 6. This nicely extends the analysis carried out in the green field case (4) and is confirmed by simulations in Section V. Note that D_t and D_r play a role analogous to d_t and d_r, respectively, in the green field case. Also, this observation suggests that additional scatterers lying between the transmit and receive array and not contributing to increased scattering angle spread will not contribute to capacity. Conversely, potential remote scatterers with significant impact on the total channel energy will increase the effective value of θ_s and quickly help build up additional capacity.
- Equation (13) suggests how, in the scattering case, the rank behavior of the MIMO channel is governed by the scattering radii and by the range, not by the physical antenna spacing. Scatterers can be viewed as virtual antenna arrays with very large spacing and aperture. Measurements of scattering radii around 100 m in typical urban settings have been reported in [13].

  The physical antenna spacing has limited impact on the capacity, unless it is very small, rendering antennas correlated, or very large so that it impacts the scattering radius itself. Antennas will remain close to uncorrelated with just $\lambda/2$ spacing for a reasonably high local angle spread/antenna beamwidth. Note that if scattering is absent at one end of the link, the relevant parameter on that particular end driving the MIMO rank becomes the antenna spacing, which then must be greatly increased in order to achieve high rank. Of course, one may use dual-polarized antennas to remove the need for scatterers, because dual-polarization tends to make the channel matrix orthogonal, but this limits the system to a capacity doubling one at most.
- When either the transmit or the receive antennas are fully correlated due to small local angle spread, the rank of the MIMO channel also drops. In this situation, the *diversity and multiplexing gains vanish*, preserving only the *receive array gain*. Note that there is no transmit array gain, since we assumed that the channel is unknown at the transmitter.
- From the above remarks, it follows that antenna correlation causes rank loss but the converse is not true. Our model is, therefore, more general than previously reported models.
- The new model contains the *product of two random Rayleigh distributed matrices*. This is in contrast with the traditional Rayleigh MIMO model of [1] and [10]. Depending on the rank of $\mathbf{R}_{\theta_S, 2D_r/S}^{1/2}$, the resulting MIMO fading statistics ranges "smoothly" from Gaussian to product of two independent Gaussians.
  - — In the HR region, $\mathbf{R}_{\theta_S, 2D_r/S}^{1/2}$ becomes an identity matrix. Using the central limit theorem, the product $\mathbf{G}_r \mathbf{G}_t$ approaches a single Rayleigh distributed matrix, which justifies the traditional model in that particular case.
  - — In the LR (i.e., rank one) region, $\mathbf{R}_{\theta_S, 2D_r/S}^{1/2}$ is the all-ones matrix. The MIMO channel becomes $\mathbf{R}_{\theta_r, d_r}^{1/2} \mathbf{g}_{rx}\, \mathbf{g}_{tx}^* \mathbf{R}_{\theta_t, d_t}^{1/2}$, an outer product of two vectors with independent transmit and receive Rayleigh fading vectors. In this case, we have no multiplexing gain, but there is still diversity gain with the exact amount depending on the transmit and receive fading correlation.

[4] $\mathbf{H}$ is normalized such that the channel energy is independent of the number of scatterers.

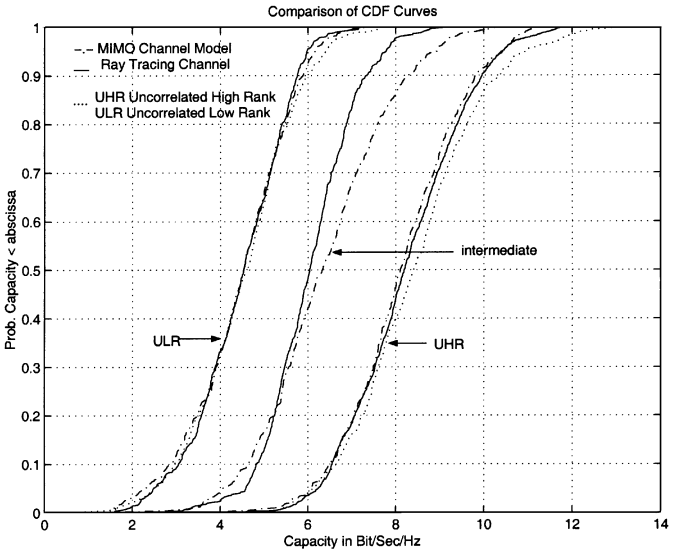

Fig. 7. Capacity cdf obtained with MIMO model for three sets of parameters. From left to right. Set 1: $D_t = D_r = 30$ m, $R = 1000$ km. Set 2: $D_t = D_r = 50$ km, $R = 50$ km. Set 3: $D_t = D_r = 100$ m, $R = 5$ km. The theoretical ULR and UHR models are plotted for comparison (dotted lines).

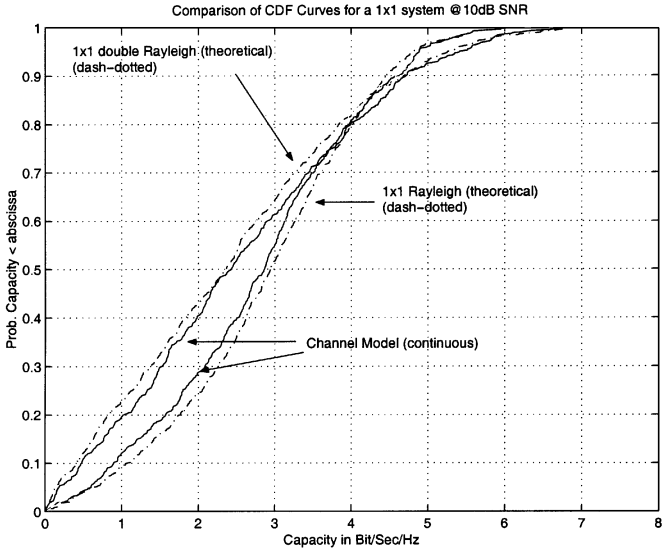

Fig. 8. Capacity cdf obtained for the 1×1 model. We use two sets of parameters from left to right. Set 1: $D_t = D_r = 30$ m, $R = 1000$ km. Set 2: $D_t = D_r = 100$ m, $R = 5$ km.

— In practice, depending on local angle spread and antenna spacing, the model will range smoothly from CLR to UHR.
— In the 1×1 case, meaningful HR and LR models can still be defined taking into account the rank of $\mathbf{R}_{\theta_S, 2D_r/S}^{1/2}$. The HR model is the traditional Rayleigh channel. The LR model has "double Rayleigh" distribution with capacity behavior worse than Rayleigh as was shown earlier.
— The model does not suggest the existence of a "correlated HR" MIMO channel, which corresponds to intuition.

V. Numerical Evaluation

In order to verify our new model, we use a comparison with an explicit ray-tracing model. In every simulation, 500 independent Monte-Carlo realizations of the ray-tracing channel are generated. The capacity distribution predicted by the proposed stochastic MIMO model for various values of the key model parameters is compared to that achieved by the actual ray tracing model with the same parameters.

The ray tracing model follows the scenario depicted in Fig. 5. In all examples, we used $S = 20$ transmit and receive scatterers which are randomly distributed around a line perpendicular to the x axis. However, we found that the final capacity results are insensitive to the particular location of the scatterers, as long as D_t, D_r and the angular spreads remain fixed. We used $M = N = 3$ and placed the scatterers at a distance R_t from the transmit array and R_r from the receive array. For simplification, we use $R_t = R_r = D_t = D_r$ in all simulations in order to maintain a high local angle spread and hence, low antenna correlation. The frequency was set to 2 GHz and the SNR was 10 dB. To introduce random fading, we use small[5] random perturbations of the transmit and receive antenna array positions in each of the Monte-Carlo experiments. The capacity distribution predicted by our channel model for the corresponding set of parameters is plotted alongside for comparison. This process was carried out for three separate sets of control parameters, covering the region between the UHR and the ULR models. The results are depicted in Fig. 7. Fig. 8 illustrates the impact of the rank of $\mathbf{R}_{\theta_S, 2D_r/S}^{1/2}$ on the capacity in the 1×1 case. The proposed channel model predicts the capacity distribution up to one b/s/Hz in all cases, and becomes almost exact as we approach UHR and ULR regions.

[5]Small enough not to affect the values of the scattering radii.

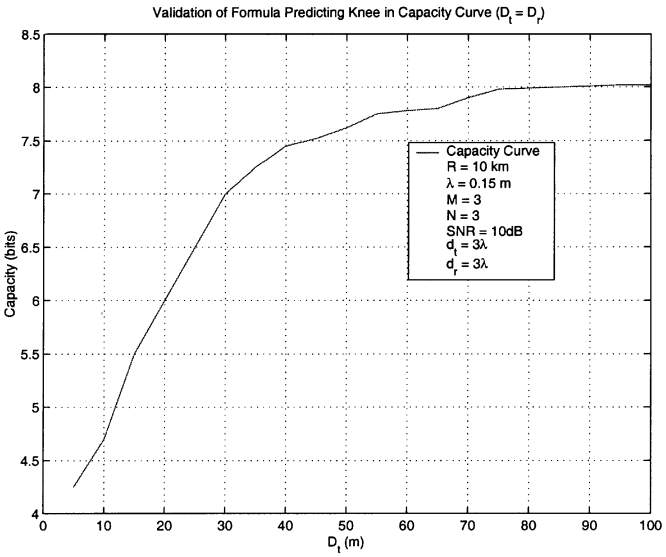

Fig. 9. Average (ergodic) capacity as a function of $D_t = D_r$. The range R is fixed to 10 km. Capacity builds up quickly as the scattering radius increases.

Finally, another validation is aimed at predicting the HR behavior of the channel using an extension of (4). Fig. 9 is a plot of ergodic (average) capacity for varying $D_t = D_r$ with R fixed at 10 km. A possible generalized HR prediction formula is

$$\frac{2D_t}{N-1}\,\frac{2D_r}{M-1} \geq \frac{R\lambda}{M} \tag{14}$$

where $2D_t/(N-1)$ can be interpreted as the maximum spacing achieved by N *virtual antennas* distributed over the distance of $2D_t$. These virtual antennas are obtained by mapping the physical antennas onto the scatterers. Similar to (4), (14) can be reinterpreted in terms of basic antenna theory as stating that the resolution of one of the two virtual arrays must be less than the angle of separation between neighboring virtual antennas on the other side. This formula predicts the HR region to start around 23 m of scattering radius, a little before but close to the knee in the figure. The result shows how capacity builds up with scattering. It also suggests that the effective aperture of the "virtual antennas" is slightly less than what is predicted by D_t. It confirms, though, that the high-capacity region is attained very easily, even for a very large range. This also provides an explanation why recent measurement campaigns in urban and suburban settings have not been able to spot pinhole channels so far.

VI. Conclusion

We introduced a model for describing the capacity behavior of outdoor MIMO channels. The new model describes the effects of certain propagation geometry parameters in LOS and fading (NLOS) situations. Moreover, it allows the study of the behavior of channel rank as a function of antenna spacing and range in LOS situations, or more practically, as a function of scattering radius and the range in fading situations. The model predicts excellent performance outdoors for very reasonable values of scattering radius, and exhibits small sensitivity of MIMO channel rank to antenna spacing. We pointed out the existence of pinhole channels for which antennas are perfectly decorrelated at the transmitter and the receiver, and yet the rank properties are poor and hence, capacity will decrease. This typically occurs for very large values of the range R. Finally, we validated our stochastic channel model through comparisons with a ray tracing model.

Appendix
Proof of the Lemma

Let $\mathbf{R}^{1/2}_{\theta_S,\,2D_r/S} = \mathbf{U}\mathbf{\Sigma}\mathbf{U}^*$ be the eigen-decomposition of $\mathbf{R}^{1/2}_{\theta_S,\,2D_r/S}$. According to (10) and (12)

$$\mathbf{Z} = \mathbf{\Phi}\mathbf{Y} = \mathbf{\Phi}\mathbf{U}\mathbf{\Sigma}\mathbf{U}^*\mathbf{G}_t\mathbf{R}^{1/2}_{\theta_t,\,d_t}. \tag{15}$$

Assuming that S is large enough and the receive scatterer positions are random (with all scatterer locations following the same distribution, and the scatterer positions varying in an independent fashion from scatterer to scatterer), the central limit theorem applied to $\mathbf{F} = \mathbf{\Phi}\mathbf{U}$ yields $[\mathbf{F}]_{m,\,s} \sim \mathcal{CN}(0,\,1)$. The correlation between the rows of $\mathbf{F}$ is governed by the receive angle spread θ_r and the antenna spacing through $\mathbf{R}_{\theta_r,\,d_r}$ [12]. The columns of $\mathbf{F}$ all have the same distribution. Furthermore, using the unitarity of $\mathbf{U}$, it follows that the columns of $\mathbf{F}$ are uncorrelated and hence, independent. We therefore have the equivalence in distribution

$$\mathbf{F} \sim \mathbf{R}^{1/2}_{\theta_r,\,d_r}\mathbf{G}_r \tag{16}$$

where $\mathbf{G}_r$ is an $M \times S$ i.i.d. Rayleigh distributed matrix. Hence, for large S, we have $\mathbf{Z} \sim \mathbf{R}^{1/2}_{\theta_r,\,d_r}\mathbf{G}_r\mathbf{\Sigma}\mathbf{U}^*\mathbf{G}_t\mathbf{R}^{1/2}_{\theta_t,\,d_t}$. Finally, the distribution of $\mathbf{G}_r$ is unchanged if we right-multiply $\mathbf{G}_r$ by the unitary matrix $\mathbf{U}$, resulting in $\mathbf{Z} \sim \mathbf{R}^{1/2}_{\theta_r,\,d_r}\mathbf{G}_r\mathbf{R}^{1/2}_{\theta_S,\,2D_r/S}\mathbf{G}_t\mathbf{R}^{1/2}_{\theta_t,\,d_t}$. □

Acknowledgment

The authors would like to thank Prof. J. Bach Andersen for his helpful comments on an earlier version of this manuscript.

References

[1] G. J. Foschini, "Layered space–time architecture for wireless communication in a fading environment when using multi-element antennas," *Bell Labs Tech. J.*, pp. 41–59, Autumn 1996.
[2] A. J. Paulraj and T. Kailath, "Increasing capacity in wireless broadcast systems using distributed transmission/directional reception," U.S. Patent no. 5 345 599, 1994.
[3] R. Müller, "A random matrix model of communication via antenna arrays," *IEEE Trans. Inform. Theory*, vol. 48, pp. 2495–2506, Sept. 2002.
[4] E. Biglieri, J. Proakis, and S. Shamai, "Fading channels: Information-theoretic and communications aspects," *IEEE Trans. Inform. Theory*, vol. 44, pp. 2619–2692, Oct. 1998.
[5] I. E. Telatar, "Capacity of multiantenna Gaussian channels," *Eur. Trans. Telecommun.*, vol. 10, no. 6, pp. 585–595, Nov./Dec. 1999.
[6] D. Chizhik, G. J. Foschini, M. J. Gans, and R. A. Valenzuela, "Keyholes, correlations, and capacities of multielement transmit and receive antennas," *IEEE Trans. Wireless Commun.*, vol. 1, pp. 361–368, Apr. 2002.
[7] J. Bach Andersen, "Array gain and capacity for known random channels with multiple element arrays at both ends," *IEEE J. Select. Areas Commun.*, vol. 18, pp. 2172–2178, Nov. 2000.
[8] G. G. Raleigh and J. M. Cioffi, "Spatio–temporal coding for wireless communication," *IEEE Trans. Commun.*, vol. 46, pp. 357–366, Mar. 1998.
[9] G. G. Raleigh and V. K. Jones, "Multivariate modulation and coding for wireless communication," *IEEE J. Select. Areas Commun.*, vol. 17, pp. 851–866, May 1999.
[10] G. J. Foschini and M. J. Gans, "On limits of wireless communications in a fading environment when using multiple antennas," *Wireless Personal Commun.*, vol. 6, pp. 311–335, 1998.
[11] "Experimental results of MIMO technology in an indoor-to-indoor environment," Gigabit Wireless Inc., Internal Tech. Rep., Mar. 1999.
[12] D. Asztély, "On antenna arrays in mobile communication systems: Fast fading and GSM base station receiver algorithms," Royal Institute of Technology, Stockholm, Sweden, Tech. Rep. IR-S3-SB-9611, Mar. 1996.
[13] J. Fuhl, A. F. Molisch, and E. Bonek, "Unified channel model for mobile radio systems with smart antennas," *Proc. IEE Radar, Sonar Navig.*, vol. 145, pp. 32–41, Feb. 1998.
[14] R. B. Ertel, P. Cardieri, K. W. Sowerby, T. S. Rappaport, and J. H. Reed, "Overview of spatial channel models for antenna array communication systems," *IEEE Pers. Commun. Mag.*, pp. 10–22, Feb. 1998.
[15] P. Driessen and G. J. Foschini, "On the capacity formula for multiple-input multiple-output wireless channels: A geometric interpretation," *IEEE Trans. Commun.*, vol. 47, pp. 173–176, Feb. 1999.
[16] J. Guey, M. Fitz, M. Bell, and W. Kuo, "Signal design for transmitter diversity wireless communication systems over Rayleigh fading channels," in *Proc. IEEE VTC*, Atlanta, GA, 1996, pp. 136–140.
[17] V. Tarokh, N. Seshadri, and A. R. Calderbank, "Space–time codes for high data rate wireless communication: Performance criterion and code construction," *IEEE Trans. Inform. Theory*, vol. 44, pp. 744–765, Mar. 1998.
[18] J. P. Kermoal, P. E. Mogensen, S. H. Jensen, J. B. Andersen, F. Frederiksen, T. B. Sorensen, and K. I. Pedersen, "Experimental investigation of multipath richness for multi-element transmit and receive antenna arrays," in *Proc. IEEE VTC Spring 2000*, vol. 3, Tokyo, Japan, 2000, pp. 2004–2008.
[19] C. C. Martin, J. H. Winters, and N. R. Sollenberger, "Multiple-input multiple-output (MIMO) radio channel measurements," in *Proc. IEEE VTC Fall 2000*, vol. 2, Boston, MA, 2000, pp. 774–779.
[20] J. Ling, D. Chizhik, P. Wolniansky, R. Valenzuela, N. Costa, and K. Huber, "Multiple transmit multiple receive (MTMR) capacity survey in Manhattan," *Electron. Lett.*, vol. 37, no. 16, pp. 1041–1042, Aug. 2001.

[21] P. Soma, D. S. Baum, V. Erceg, R. Krishnamoorthy, and A. J. Paulraj, "Analysis and modeling of multiple-input multiple-output (MIMO) radio channel based on outdoor measurements conducted at 2.5 GHz for fixed BWA applications," in *Proc. IEEE Int. Conf. Communications (ICC)*, vol. 1, New York, NY, 2002, pp. 272–276.
[22] D. Shiu, G. J. Foschini, M. J. Gans, and J. M. Kahn, "Fading correlation and its effect on the capacity of multi-element antenna systems," *IEEE Trans. Commun.*, vol. 48, pp. 502–513, Mar. 2000.
[23] S. L. Loyka, "Channel capacity of MIMO architecture using the exponential correlation matrix," *IEEE Commun. Lett.*, vol. 5, pp. 369–371, Sept. 2001.
[24] D. Chizhik, G. Foschini, and R. A. Valenzuela, "Capacities of multi-element transmit and receive antennas: Correlations and keyholes," *Electron. Lett.*, pp. 1099–1100, 2000.
[25] D. Johnson and D. Dudgeon, *Array Signal Processing*. Englewood Cliffs, NJ: Prentice-Hall, 1993.
[26] G. D. Golden, G. J. Foschini, R. A. Valenzuela, and P. W. Wolniansky, "Detection algorithm and initial laboratory results using the V-BLAST space–time communication architecture," *Electron. Lett.*, vol. 35, no. 1, pp. 14–15, Jan. 1999.
[27] H. Bölcskei, D. Gesbert, and A. J. Paulraj, "On the capacity of OFDM-based spatial multiplexing systems," *IEEE Trans. Commun.*, vol. 50, pp. 225–234, Feb. 2002.
[28] H. Bölcskei and A. J. Paulraj, "Space-frequency coded broadband OFDM systems," in *Proc. IEEE WCNC*, vol. 1, Chicago, IL, Sept. 2000, pp. 1–6.

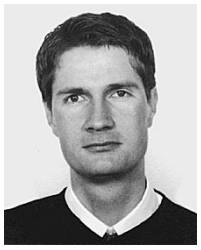

David Gesbert (S'96–M'99) received the Ph.D. degree from Ecole Nationale Superieure des Telecommunications (ENST), Paris, France, 1997.

From 1993 to 1997, he was with France Telecom Research (CNET), Radio Systems Department, Paris. From April 1997 to October 1998, he was a Postdoctoral Fellow in the Information Systems Laboratory, Stanford University, Stanford, CA. In October 1998, he took part in the founding team of Iospan Wireless, Inc., formerly Gigabit Wireless, Inc., San Jose, CA. In 2001, he became an independent consultant and joined in parallel the Signal Processing Group, Department of Informatics, University of Oslo, Oslo, Norway, as an Adjunct Associate Professor. He is the author of over 40 papers and 15 patents, granted or pending, in the area of wireless systems. His research interests are in the area of high-speed wireless data/IP networks, smart antennas and MIMO, and link layer and system optimization.

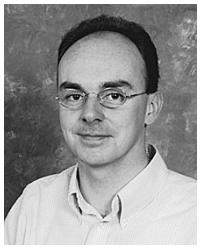

Helmut Bölcskei (M'98) was born in Mödling, Austria, on May 29, 1970. He received the Dipl.-Ing. and Dr. techn. degrees in electrical engineering/communications from Vienna University of Technology, Vienna, Austria, in 1994 and 1997, respectively.

From 1994 to 2001, he was with the Institute of Communications and Radio-Frequency Engineering, Vienna University of Technology. From March 2001 to January 2002, he was an Assistant Professor of Electrical Engineering at the University of Illinois at Urbana-Champaign. Since February 2002, he has been an Assistant Professor of Communication Theory at ETH Zürich, Switzerland. From February to May 1996, he was a Visiting Researcher at Philips Research Laboratories, Eindhoven, The Netherlands. From February to March 1998, he visited the Signal and Image Processing Department at ENST Paris, France. From February 1999 to February 2001, he was an Erwin Schrödinger Fellow of the Austrian National Science Foundation (FWF) performing research in the Smart Antennas Research Group in the Information Systems Laboratory, Department of Electrical Engineering, Stanford University, Stanford, CA. From 1999 to 2001, he was a consultant for Iospan Wireless, Inc. (formerly Gigabit Wireless, Inc.), San Jose, CA. His research interests include communication and information theory and statistical signal processing with special emphasis on wireless communications, MIMO antenna systems, space–time coding, orthogonal frequency-division multiplexing, and wireless networks.

Dr. Bölcskei received a 2001 IEEE Signal Processing Society Young Author Paper Award and serves as an Associate Editor for the IEEE TRANSACTIONS ON SIGNAL PROCESSING.

Dhananjay A. Gore was born in Bombay, India, on January 8, 1977. He received the B.Tech. degree in electrical engineering from the Indian Institute of Technology, Bombay (IITB), India, in 1998 and the M.S. degree in electrical engineering from Stanford University, Stanford, CA, in 2000.

He is currently pursuing the doctoral degree in the Smart Antennas Research Group at Stanford University. His research interests are in the areas of wireless communications and MIMO antenna systems.

Mr. Gore is a recipient of the Institute Silver Medal from IITB and the School of Engineering Fellowship from Stanford University.

Arogyaswami J. Paulraj (SM'85–F'91) received the Ph.D. degree from the Naval Engineering College and Indian Institute of Technology, Bangalore, in 1973.

He has been a Professor at the Department of Electrical Engineering, Stanford University, Stanford, CA, since 1993, where he supervises the Smart Antennas Research Group. This group consists of approximately 12 researchers working on applications of space–time signal processing for wireless communications networks. His research group has developed many key fundamentals of this new field and helped shape a worldwide research and development focus onto this technology. His nonacademic positions included Head, Sonar Division, Naval Oceanographic Laboratory, Cochin, India; Director, Center for Artificial Intelligence and Robotics, Bangalore; Director, Center for Development of Advanced Computing; Chief Scientist, Bharat Electronics, Bangalore, and Chief Technical Officer and Founder, Iospan Wireless, Inc., San Jose, CA. He has also held visiting appointments at Indian Institute of Technology, Delhi, Loughborough University of Technology, and Stanford University. He sits on several boards of directors and advisory boards for U.S. and Indian companies/venture partnerships. His research has spanned several disciplines, emphasizing estimation theory, sensor signal processing, parallel computer architectures/algorithms and space–time wireless communications. His engineering experience included development of sonar systems, massively parallel computers, and more recently broad-band wireless systems. He is the author of over 250 research papers and holds eight patents.

Dr. Paulraj has won several awards for his engineering and research contributions. These include two President of India Medals, the CNS Medal, the Jain Medal, the Distinguished Service Medal, the Most Distinguished Service Medal, the VASVIK Medal, and the IEEE Best Paper Award (Joint), amongst others. He is a member of the Indian National Academy of Engineering.